

Electronic and spin transport properties of zigzag graphene nanoribbon mediated by metal adatom: QUAMBO-NEGF approach

G. P. Zhang^{1,2}, Xiaojie Liu^{3,1}, C. Z. Wang¹, Y. X. Yao¹, W. C. Lu^{3,4} and K. M. Ho¹

¹*Ames Laboratory, U. S. Department of Energy,
and Department of Physics and Astronomy, Iowa State University, Ames, IA 50011, USA*

²*Department of Physics, Renmin University of China, Beijing 100872, China*

³*Laboratory of Theoretical and Computational Chemistry, Institute of Theoretical Chemistry,
Jilin University, Changchun, Jilin 130021, P. R. China and*

⁴*College of Physics, and Laboratory of Fiber Materials and Modern Textile,
the Growing Base for State Key Laboratory, Qingdao University, Qingdao, Shandong 266071, P. R. China**

(Dated: November 21, 2018)

Electronic and spin transport properties of zigzag graphene nanoribbon (ZGNR) with alkali-, group-III and 3d-transition-metal adatoms on the hollow center are investigated by quasi-atomic minimal basis orbits (QUAMBOs), a first-principles tight binding (TB) scheme, combined with non-equilibrium Green's function (NEGF). QUAMBOs-TB parameters of carbon atoms in the middle scattering region are constructed by divide-and-conquer approach. It is found that the transmission is generally reduced by metal adatom, which can be well explained by the geometry of π -orbital and the corresponding interaction strength between π -orbital and metal adatom. Naturally, the transport at the Fermi level is not sensitive to metal adatom because of weak interaction between the localized edge state and metal adatom. Spin transport near the Fermi level is induced by Co, Fe and V adatom, and higher than 50% transmission spin polarization with a board energy window around 0.34eV, 0.36eV and 0.56eV respectively. Thereinto, a higher transmission of one spin state is originated from a less distortion of the corresponding π -orbital by metal adatom rather than high DOS of this spin state. Further the effect of the width of ZGNR on electronic and spin transport properties is discussed.

PACS numbers: 72.80.Vp, 73.20.At, 31.15.A-

I. I. INTRODUCTION

Graphene [1], a true two-dimensional crystalline lattice formed by carbon atoms, has attracted tremendous interest in physics, chemistry, and material science. The novel electronic structures of graphene with a linear dispersion relation near the Dirac point generate unusual transport properties [1–7], such as the conductivity linear with the gate voltage resulting from the linear spectrum [1, 2], unconventional integer quantum Hall effect [3, 4], and high carrier mobility [5] which make graphene as a good candidate in electronic devices. In addition, there have been a lot of interests in modifying the electronic, spintronics, transport, as well as magnetic properties of graphene through adsorption of various atoms and molecules on graphene interacting with graphene sheet [8–11]. Similar to the proposal of biosensor by Schedin et al. [12], it was observed gate-tunable spin transport in graphene at room temperature [13–15]. First principle investigation of the effects of metal contact on graphene [16, 17] was stimulated by the metallic contacts in the transport measurement. On the other hand, the effect of adatom, dimmer and atom-chain of transition metal on electronic and spin transport had also been explored [18–20].

Due to the huge computational demand for first principle calculation of large scale system, lot of efforts had

been made to extract tight binding parameters from first principle calculation [17, 21]. Recently quasi-atomic minimal basis set orbitals (QUAMBOs) was developed by Yao et al., in which TB Hamiltonian and overlap matrices of a given system can be accurately extracted from ab initio calculations without any fitting procedures [22, 23]. Furthermore, QUAMBOs scheme enables the application of divide-and-conquer approach benefitted from the dependence of local environment of QUAMBOs-TB parameters as shown in Refs. [22, 24]. On this basis, non-equilibrium Green's function (NEGF) method combined with Landauer' formalism [25–27] are preformed to calculate the electronic transport. Therefore such a QUAMBO-NEGF scheme can be applied to study the electronic transport in large atomistic systems without sacrificing the accuracy [24].

Our previous work investigated the bond and charge transfer between various metal adatom, including alkali-, group-III and 3d-transition-metal adatom, and graphene system [10]. In this letter, we further investigate the electronic and spin transport through ZGNR in the presence of these metal adatoms by QUAMBO-NEGF scheme. There are two distinct differences between our work and previous similar works [18, 20]. One is that spin unpolarized basis is adopted in our first-principles calculation of ideal ZGNR [24, 28], since the ground state of ZGNR under spin polarized basis is not stable at finite temperature. Certainly, for graphene with metal adatom as shown in Fig. 1, spin polarized basis should

*wangcz@ameslab.gov(C. Z. Wang) and liuxj82@gmail.com(X. J. Liu) be used in first-principles calculation [10]. The other

is that the Fermi level of the middle scattering region is shifted to zero [18, 20]. However, here TB parameters near the interfaces equal to the counterparts at the leads, in order to be consistent with the screening of metal adatom at the interface, and therefore the Fermi level of the middle scattering region may not be shifted to zero. Though above differences and different width of ZGNR, the trends of electron current with a certain dominant spin state [18, 20] are consistent with our work. We find that the current with a certain dominant spin state is originated from a less distortion of the corresponding π -orbit by metal adatom. Furthermore, a divide-and-conquer approach is adopted to construct QUAMBOs-TB parameters for ZGNR with metal adatom on hollow center, which goes beyond the construction of QUAMBOs-TB parameters in the presence of one type of atom [28].

This paper is arranged as follows. In Sec. 2, we present the VASP calculation details and formula of the transmission and density of states based on QUAMBO-TB Hamiltonian and overlap matrices; in Sec. 3, we describe the reconstruction of TB parameters for zigzag graphene nanoribbon (ZGNR) with various metal adatoms and investigate the effect of metal adatom and the width of ZGNR on electronic and spin transport properties; and finally we give a brief summary in Sec. 4. In our investigation, the transmission is reduced by metal adatom and is well explained by density of states, the distortion of QUAMBOs-TB parameters by metal adatom, the geometry of π -orbit and then the interaction between π -orbit and metal adatom. in sections V and VI.

II. COMPUTATIONAL DETAILS

The first-principles calculations are performed based on the density functional theory (DFT) with generalized gradient approximation (GGA) in the form of PBE (Perdew-Burke-Ernzerhof) [29] implemented in the VASP [30–32] (Vienna Ab initio Simulation Package) code, including spin polarization and dipole moment corrections [33, 34]. Valence electrons are treated explicitly and their interactions with ionic cores are described by PAW (Projector Augmented Wave) pseudopotentials [35, 36]. The wave functions are expanded in a plane wave basis set with an energy cutoff of 600 eV. A k-point sampling of $6 \times 6 \times 1$ Monkhorst-Pack grids in the first Brillouin zone of the supercell and a Gaussian smearing with a width of 0.05 eV is used in the calculations. All atoms in the supercell are allowed to relax until the forces on each atom are smaller than $0.01 \text{ eV}/\text{\AA}$. The supercell dimensions are kept fixed during the relaxation.

The adatom/graphene system is modeled by having one adatom in a 4×4 parallelogram graphene supercell with periodic boundary conditions as shown in Fig. 1. The primitive cell of graphene is a parallelogram with two carbon atoms. The lattice constant obtained from our calculation is 2.46\AA , agrees well with experimental

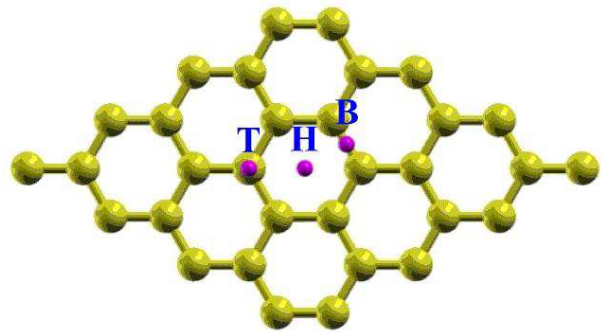


FIG. 1: (Color online) Three adsorption sites for an adatom on graphene: hollow center (H), bridge center (B), and top (T) sites in a periodic 4×4 graphene supercell. In first-principles calculation, H site is stable for metal adatom adsorbed on the graphene.

value. The dimension of the supercell in the z direction is 15\AA , which allows a vacuum region of about 12\AA to separate the atoms in the supercell and their replicas. Usually there are three typical sites for adatoms positioned on graphene at the top of a carbon atom, labeled top (T) site, at the middle of a carbon-carbon bond, labeled bridge (B) site, and at the hexagonal center site, labeled hollow (H) site, respectively, as indicated in Fig. 1. In our calculations, H site is stable for metal adatoms adsorbed on the graphene under study.

Using the self-consistent wave functions from the plane-wave basis VASP calculations, a set of structure-dependent quasi-atomic minimal basis orbitals (QUAMBOs) for each adatom/graphene system is constructed following the scheme developed previously [22, 23]. While highly localized on atoms and exhibiting shapes close to the orbitals of the isolated atoms, the QUAMBOs span exactly the same occupied subspace as the wave functions determined by the first-principles calculations with a large plane-wave basis set. The Hamiltonian and overlap matrices in the QUAMBOs representation give exactly the same energy bands and wave functions of the occupied electronic states as those obtained by the fully converged first-principles calculations using the VASP [10, 22, 23]. Therefore, using the wave functions from the VASP calculations, accurate tight-binding (TB) Hamiltonian and overlap matrix elements are calculated by QUAMBO approach [22, 23]. The electronic transmission probability in such systems can be calculated as:

$$T_{\sigma}(E) = \text{Tr}[\Gamma_{L,\sigma}(E)G_{\sigma}^R(E)\Gamma_{R,\sigma}(E)G_{\sigma}^A(E)], \quad (1)$$

$$\Gamma_{L,\sigma}(E) = i\left[\sum_{L,\sigma}^R(E) - \sum_{L,\sigma}^A(E)\right]. \quad (2)$$

Here $\Gamma_{L,\sigma}(E)$ is the coupling function of left semi-infinite lead (L , ZGNR on the left of Fig. 2b), and $\sum_{L,\sigma}^A(E)$ is the conjugate of the advanced self energy $\sum_{L,\sigma}^R(E)$.

$\sum_{L,\sigma}^R(E)$ is calculated through surface Green's function iteratively [25–27],

$$\sum_{L,\sigma}^R(E) = (H_{LM\sigma} - ES_{LM\sigma})g_{L,\sigma}^R \left(H_{LM\sigma}^\dagger - ES_{LM\sigma}^\dagger \right), \quad (3)$$

In the present calculation, whether the spin state indexed by σ is degenerate or not depends on the adsorbed metal adatom on ZGNR. M and R stand for the middle scattering region and the right lead respectively. $g_{L,\sigma}^R$ is the surface Green's function of the left lead. $H_{LM\sigma}$ ($S_{LM\sigma}$) is the Hamiltonian (overlap) matrix between left lead and the middle scattering region. The same calculation can also be performed for the right lead to obtain $\sum_{R,\sigma}^R(E)$. The retarded Green's function is calculated by

$$G_\sigma^R(E) = \left(ES_{M,\sigma} - H_{M,\sigma} - \sum_{L,\sigma}^R(E) - \sum_{R,\sigma}^R(E) \right)^{-1}, \quad (4)$$

where $H_{M,\sigma}$ ($S_{M,\sigma}$) is the Hamiltonian (overlap) matrix of the middle scattering region. E is the energy for electron injecting from left reservoir. $E = 0$ implies that the Fermi energies of leads have been shifted to zero, while the Fermi energy of the middle scattering region has not been shifted to zero due to the presence of metal adatom. We stress that the conductance of system is under zero bias between left and right leads. Meanwhile, the density of states (DOS) $\rho_\sigma(E) = -\text{ImTr} [G_\sigma^R(E)S_{M,\sigma}] / \pi$ in open boundary system of lead-middle scattering region-lead should be different from DOS in periodic boundary system by first-principle calculation.

III. RESULT AND DISCUSSION

A. Reconstruction of TB parameters for ZGNR with metal adatom on the hollow center by divide-and-conquer approach

In order to study the transport property of zigzag graphene nanoribbon (ZGNR) with various metal adatom adsorbed at the hollow center, we choose a general structure of lead-middle scattering region-lead as shown in Fig. 2(b,c). The lead and the middle scattering region are a semi-infinite ZGNR and a ZGNR with metal adatom respectively. To construct the middle part, we at first reshape the structure as shown in Fig. 1, into a rectangle as shown in Fig. 2(a), and then replace the center part of ZGNR in the middle scattering region by this rectangle. The feasibility of this reconstruction scheme is assured by the local environment dependence of TB parameters obtained by QUAMBOs as the example of carbon atom chain between ZGNR was represented in Ref. [28]. Here we check the screening effect of metal adatom at lead-middle scattering region interface and find that the TB parameters of carbon atoms are slightly distorted

by metal adatom, except for those of six carbon atoms close to metal adatom, as shown in Fig. 3(b). The local environment dependence enables us to easily construct a wider system and estimate the effect of the width of ZGNR lead on transport property.

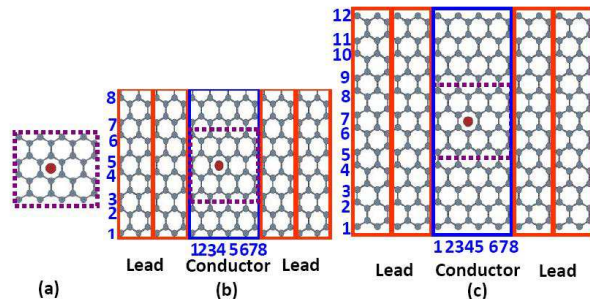


FIG. 2: (Color online) (a) The periodic 4×4 graphene supercell shown in Fig. 1 is arranged into a rectangle shape. (b-c) The middle scattering region in the blue frame, i.e., the conductor part, is composed by zigzag graphene nanoribbon (ZGNR) with an metal adatom at the hollow center. Passivating hydrogen atoms at the edges of ZGNR are not shown. The primitive unit (PU) of ZGNR lead is in the red frame. The width of ZGNR W is 8 and 12 in (b) and (c) respectively.

Magnetism in graphene is induced by 3d transition metal, such as Co, Fe and V. In this case, TB parameters indexed by spin up and down indices are not degenerate due to the induced magnetism in graphene sheet, as an example in the presence of Co adatom shown in Fig. 3(b). Thereinto, spin splitting effect is strongest for six carbon atoms closest to these metal adatoms as shown in Fig. 3(a). However, this kind of spin splitting effect is slight for those carbon atoms far away from these metal adatoms. Therefore it is reliable to retain spin-degenerate QUAMBO-TB parameters for those carbon atoms close to the zigzag edge in the middle scattering region.

B. Electronic and spin transport properties in the presence of metal adatom and comparison with some other published works

For ideal ZGNR with $W=8$ (here W being the number of carbon atoms in one arrow as shown in Fig.2b), the transmission is quantized, as shown in Fig. 4(a). However the transmission around a narrow region of Fermi level with the width of 0.04eV is larger than 1, similar to the transmission in Ref. [37]. QUAMBOs-TB parameters are reliable as one perfect transmission for the energy range $[-1.06\text{eV}, 1.24\text{eV}]$ with a width of 2.30eV is well reproduced, as shown in Fig. 4(a). We plot the spatial density of states (SDOS) of each carbon atom at $E=-1, -0.6, 0, 0.6$ and 1 eV in Fig. 5(a-e). It is found that high SDOS horizontally distributes at the center of ZGNR as E is less than 0, and high SDOS moves toward the zigzag

edge little by little and finally an edge state occurs when E approaches 0. On the contrary, SDOS vertically distributes when E is larger than 0. Therefore the geometry of π -orbit determines the interaction strength between π -orbit and metal adatom and then transport properties through ZGNR.

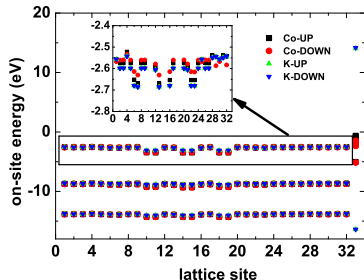
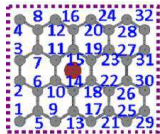


FIG. 3: (Color online) (a) Ordering for carbon atoms in rectangle shape as shown in Fig. 2(a). (b) On-site energies of carbon atom in the presence of Co and K adatom. π -orbitals of six carbon atoms closest to the metal adatom (i.e. carbon # 10, 11, 14, 15, 18 and 19) are strongly affected by the metal adatom, while π -orbitals of other carbon atoms are slightly distorted. The local-environment dependence of TB parameters enables the reconstruction of middle scattering region as shown in Fig. 2.

The transport properties of ZGNR with various metal adatom are shown in Fig. 4(a-b,d-f). It is found that the transmission may be spin-independent as shown in Fig. 4(a-b) and spin-dependent as shown in Fig. 4(d-f), which depends on the net magnetism induced by metal adatom. First of all, we discuss the spin-independent transport. It is found that the transmission within the energy range $[-2.0\text{eV}, -0.02\text{eV}]$ is greatly reduced by the distortion of metal adatom. Thereinto, the perfect channel within $[-1.06\text{eV}, -0.02\text{eV}]$ for ideal ZGNR with $W=8$ is blocked, which is embodied in localized SDOS at the conductor-lead interfaces as shown in Fig. 5(f-g), as π -orbit with high SDOS distributing horizontally in the center interacts strongly with metal adatom on hollow center. However, the perfect channel within $[0.02\text{eV}, 1.24\text{eV}]$ remains a finite transmission in the presence of metal adatom, since low SDOS is in the vicinity of metal adatom and then a weak interaction occurs between metal adatom and π -orbit as shown in Fig. 5(i-j). It can be inferred that the finite transmission in this energy range is originated from the unchanged geometry of SDOS, though

SDOS is distorted by metal adatom. It is well understood that the transmission at the Fermi level $E=0$ is not altered in the presence of various metal adatom, since the edge state close to zigzag edge is far away from the metal adatom and then weakly interacts with metal adatom. Its corresponding SDOS shows that the edge state has not been distorted by the metal adatom as shown in Fig. 5(h).

It is interesting that the transmission curves collapse as the energy ranges from $[-2.0\text{eV}, 1.24\text{eV}]$ in the presence of Al, In, K and Na, as shown in Fig. 4(a). The transmission curve within the energy range $[-2.0\text{eV}, 1.24\text{eV}]$ in the presence of Ni adatom almost collapses with those mediated by Al and K adatoms, as shown in Fig. 4(b). Different from the above four metal adatoms, Ni adatom provides two transmission peaks at -0.94eV and -0.34eV as a result of peaks in high density of states (DOS), as shown in Fig. 4(c). As the energy is lower than -1.75eV , the transmission is not sensitive to metal adatoms, since π -orbit has a weak interaction with metal adatom. As the energy is higher than 1.24eV , spin-independent transport mediated by metal adatom shows three different trends as shown in Fig. 4(a) and 4(b). This is induced by the types of metal adatoms, (1) alkali-metal Al and In, (2) group-III metal K and Na, and (3) 3d transition-metal Ni. Their corresponding outer electron structures are $3s^23p^1$, $5s^25p^1$, $3s^1$, $4s^1$ and $3d^84s^2$ respectively. It shows that the transport at high energy is determined by the outer electron structure of metal adatoms. We should stress that Ni/graphene system has no net magnetic moment due to charge transfer from Ni adatom to graphene, though isolated Ni atom has of magnetic moment [10]. Consequently, the transmission is spin-degenerate in the presence of Ni adatom on ZGNR.

The spin splitting in transport is obvious within the energy range near Fermi level once there is magnetism induced in graphene sheet by transition metal adatom, i.e. Co, Fe and V. However, no spin splitting presents in transmission for the energy far away from the Fermi level, which applies that magnetism mainly originates from π -orbit consistent with DOS from first-principles calculation. In the presence of Co adatom, the transmission for electron with spin down (Tdown) within the energy range $[0.02, 1.0]\text{eV}$ is higher than the transmission for electron with spin up (Tup). Meanwhile, its density of states (DOS) for electron with spin down is lower than the opposite within the above energy range, as shown in Fig. 4(d). Therefore, a high transmission for electron with spin down is due to less distortion of π -orbit indexed by spin down. This conclusion is also embodied in the less distortion of the on-site energy indexed by spin down in the presence of Co adatom as shown in Fig. 3(b). The relation between the distortion and the transmission in the above applies to all non-degenerate spin transport in the presence of other transition metal adatoms Co and V as shown in Fig. 4(e-f). It is found that the transmission curve within the energy range $[-2, 1.24]\text{eV}$ collapses with that mediated by Al adatom, when the spin state results

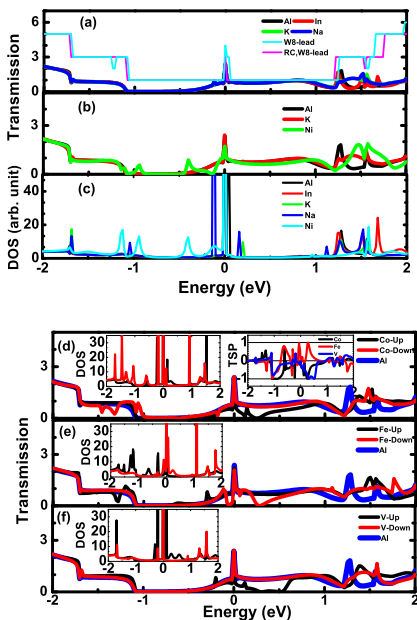


FIG. 4: (Color online) Transmission versus the energy through ZGNR in the presence of (a) Al, In, K and Na adatom and (b) Al, K and Ni adatoms adsorbed on the hollow center of ZGNR. Curves of the transmission versus the energy for exact versus reconstructed ZGNR are plotted in (a). "RC, W8-lead" stands for reconstructed ZGNR [22, 28]. (c) Density of states (DOS) versus the energy for ZGNR with Al, In, K, Na and Ni adatoms. (d-f) show transmission for electron with spin-up and spin-down indices and the corresponding DOS versus the energy through ZGNR in the presence of Co, Fe and V adatom respectively. Transmission spin polarization (TSP) in the presence of Co, Fe and V adatom is shown in the right inset of (d). The transmission in the presence of Al adatom is plotted in (d-f) for comparison. The width of ZGNR is $W=8$.

in a less distortion to π -orbit, as shown in Fig. 4(d-f). We also investigate the transmission spin polarization (TSP), which is defined as $(T_{up}-T_{down})/(T_{up}+T_{down})$. Current with spin up (down) dominates when TSP is positive (negative). In view of the transmission and TSP, the energy range with a range width of 0.34eV, 0.36eV and 0.56eV above the Fermi level is suitable for spin manipulation mediated by Co, Fe and V respectively, where the absolute value of TSP is larger than 0.5. As we discuss above, the transmission at the energy higher than 1.24eV sensitively depends on the outer electron structure of metal adatom.

As we mentioned in the introduction, in other similar works on transport property of ZGNR in the presence of metal adatom, the Fermi level of the middle scattering region is shifted to zero [18, 20]. Furthermore, ZGNR lead has a gap when spin polarized basis is chosen, therefore the transmission near the Fermi level is zero for ZGNR with Co adsorbed on the hollow center [18]. Similarly, it was found that a single Fe atom adsorbed on ZGNR

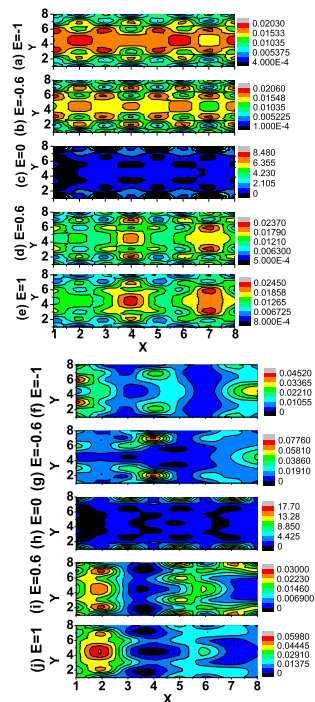


FIG. 5: Spatial density of states (SDOS) of each carbon atom in (a-e) pure ZGNR and (f-j) ZGNR with Al metal adatom on hollow center. SDOS mainly comes from π -orbit of carbon atoms. The width of ZGNR W is 8.

could not induce a finite transmission around the Fermi level [20]. Though different basis adopted in calculation and different width of ZGNR from our work was chosen, it was found that the electron with spin down (spin up) in the presence of Co (Fe) adatom provides a higher transmission within some certain energy ranges [18, 20], which is consistent with our work.

C. Effect of the width of ZGNR lead on electronic and spin transport

The trend of the effect of ZGNR lead on electronic and spin transport is highly desired, as electronic devices are usually wider than the system under study. However, it is difficult to include a wide ZGNR lead in first-principles calculation due to time and memory consuming. We continue to adopt divide-and-conquer approach to construct a ZGNR lead with $W=12$. The comparison of the transmission for two pure ZGNR leads is shown in Fig. 6(a). The transmission is quantized for pure leads, where the quantity of transmission depends on the number of eigenchannels available for the certain energy. Since the wider lead provides more channels for electronic transport, therefore the energy range for each quantized transmission becomes narrower as the width of ZGNR increases.

ZGNR with Co adatom on the hollow center is chosen

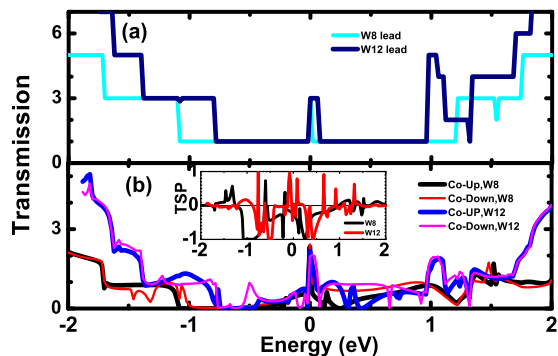


FIG. 6: ((Color online) (a) Transmission versus energy through ZGNR leads with $W=8$ and $W=12$. (b) The transmission and transmission spin polarization (TSP, shown in the inset) through ZGNR in the presence of Co adatom as the width of ZGNR W is 8 and 12 respectively.

as an example to estimate the effect of ZGNR on electronic and spin transport as shown in Fig. 6(b). The curve of the transmission versus the energy in the case of $W=12$ ZGNR lead is similar to the counterpart in the case of $W=8$ ZGNR lead, in which the transmission increases with the absolute value of the energy except for those energy ranges with no transmission at all. The difference between two cases is that wider ZGNR provides more channels for electronic transport and therefore the transmission is generally higher, except for those energy ranges with no transmission at all. We also investigate the behavior of TSP versus the energy and find that the energy range corresponding to a finite TSP becomes narrower and closer to the Fermi level as the width of ZGNR increases. Similarly, taken into account a finite transmission, the energy range $[0.3, 0.52]$ eV is suitable for

spin manipulation, in which the absolute value of TSP is larger than 0.5, as the width of ZGNR lead is $W=12$. It is found that not only the effect of spin splitting but the effect of width of ZGNR lead on the transmission at $E=0$ is negligible. As we discussed above, this phenomenon occurs because the edge state localized at the zigzag edge is slightly distorted by the metal adatom.

IV. IV. SUMMARY

Electronic and spin transport properties of metal adatom adsorbed on zigzag graphene nanoribbon (ZGNR) are investigated by QUAMBO-NEGF combined with divide-and-conquer approach. The effect of metal adatom on the transmission has been investigated. Non-degenerate spin transport near the Fermi level is induced by transition metal adatom such as Co, Fe and V. Spin manipulation has also been analyzed in term of transmission spin polarization. Further the trend of the electronic and spin transport properties through a wider ZGNR lead is discussed.

V. ACKNOWLEDGEMENTS

Work at Ames Laboratory was supported by the US Department of Energy, Basic Energy Sciences, Division of Materials Science and Engineering including a grant of computer time at the National Energy Research Supercomputing Center (NERSC) in Berkeley, under Contract No. DE-AC02-07CH11358. X. J. Liu acknowledged the support from China Scholarship Council (File NO.2009617104) and W. C. Lu acknowledged the National Natural Science Foundation of China (Grant No.20773047 and No.21043001).

-
- [1] K. S. Novoselov, et al., *Science* **306**, 666 (2004).
[2] K. S. Novoselov, et al., *Nature (London)* **438**, 197 (2005).
[3] V. P. Gusynin, and S. G. Sharapov, *Phys. Rev. Lett.* **95**, 146801 (2005).
[4] Y. Zhang, Y. Tan, H. L. Stormer, and P. Kim, *Nature* **438**, 201 (2005).
[5] A. K. Geim, and K. S. Novoselov, *Nature Material* **6**, 183 (2007).
[6] K. Pi et al., *Phys. Rev. Lett.* **104**, 187201 (2010).
[7] Z. Zanolli, G. Onida, and J. C. Charlier, *ACS NANO* **4**, 5174 (2010).
[8] K. T. Chan, J. B. Neaton, and M. L. Cohen, *Phys. Rev. B* **77**, 235430 (2008).
[9] X. Liu, C. Z. Wang, M. Hupalo, Y. X. Yao, M. C. Tringides, W. C. Lu, and K. M. Ho, *Phys. Rev. B* **82**, 245408 (2010).
[10] X. Liu, C. Z. Wang, Y. X. Yao, W. C. Lu, M. Hupalo, M. C. Tringides, and K. M. Ho, *Phys. Rev. B* **83**, 235411 (2011).
[11] M. Hupalo, X. Liu, C. Z. Wang, W. C. Lu, Y. X. Yao, K. M. Ho, and M. C. Tringides, *Advanced Materials* **23**, 2082 (2011).
[12] F. Schedin et al., *Nature Material* **6**, 652 (2007).
[13] N. Tombros et al., *Nature (London)* **448**, 571 (2007).
[14] S. Cho, Y.-F. Chen, and M. S. Fuhrer, *Appl. Phys. Lett.* **91**, 123105 (2007).
[15] W. Han et al., *Phys. Rev. Lett.* **102**, 137205 (2009).
[16] G. Giovannetti, P. A. Khomyakov, G. Brocks, et al, *Phys. Rev. Lett.* **101**, 026803 (2008).
[17] S. Barraza-Lopez, M. Vanević, M. Kindermann, and M. Y. Chou, *Phys. Rev. Lett.* **104**, 076807 (2010).
[18] Cocchi C et al, *J. Chem. Phys.* **133**, 124703 (2010).
[19] Cao C et al, *Phys. Rev. B* **81**, 205424 (2010).
[20] Zhang Z L et al, *J Phys. D: Appl. Phys.* **44**, 215403 (2011).
[21] A. Urban, M. Reese, M. Mrovec, C. Elsässer, and B.

- Meyer, Phys. Rev. B **84**, 155119 (2011).
- [22] Y. X. Yao et al., J. Phys. Condens. Matter **21**, 235501 (2009).
- [23] C. Z. Wang et al., Sci. Model. Simul. **15**, 81 (2008).
- [24] X. W. Fang et al, Phys. Lett. A **375**, 3710 (2011).
- [25] M. B. Nardelli, and J. Bernholc, Phys. Rev. B **60**, R16338 (1999).
- [26] M. B. Nardelli, Phys. Rev. B **60**, 7828 (1999).
- [27] M. P. L. Sancho, J. M. L. Sancho, and J. Rubio, J. Phys. F **14**, 1205 (1984); J. Phys. F **15**, 851 (1985); J. Phys. C: Solid State Phys. **18**, 1803 (1985).
- [28] G. P. Zhang et al., J. Phys.: Condens. Matter **23**, 025302 (2011).
- [29] J. P. Perdew, K. Burke, and M. Ernzerhof, Phys. Rev. Lett. **77**, 3865 (1996).
- [30] G. Kresse, and J. Furthmüller, Comput. Mater. Sci. **6**, 15 (1996).
- [31] G. Kresse, and J. Hafner, Phys. Rev. B **47**, 558 (1993).
- [32] G. Kresse, and J. Furthmüller, Phys. Rev. B **54**, 11169 (1996).
- [33] G. Makov, and M. C. Payne, Phys. Rev. B **51**, 4014 (1995).
- [34] J. Neugebauer, and M. Scheffler, Phys. Rev. B **46**, 16067 (1992).
- [35] P. E. Blöchl, Phys. Rev. B **50**, 17953 (1994).
- [36] G. Kresse, and D. Joubert, Phys. Rev. B **59**, 1758 (1999).
- [37] L. A. Agapito, and Hai-Ping Cheng, J. Phys. Chem. C **111**, 14266 (2007).